SIAM J. NUMER. ANAL.
Vol. 56, No. 4, pp. 2322–2344

COMPUTING EFFECTIVE DIFFUSIVITY OF CHAOTIC AND STOCHASTIC FLOWS USING STRUCTURE-PRESERVING SCHEMES*

ZHONGJIAN WANG†, JACK XIN‡, AND ZHIWEN ZHANG§

Abstract. In this paper, we study the problem of computing the effective diffusivity for a particle moving in chaotic and stochastic flows. In addition, we numerically investigate the residual diffusion phenomenon in chaotic advection. The residual diffusion refers to the nonzero effective (homogenized) diffusion in the limit of zero molecular diffusion as a result of chaotic mixing of the streamlines. In this limit, traditional numerical methods typically fail since the solutions of the advection-diffusion equations develop sharp gradients. Instead of solving the Fokker–Planck equation in the Eulerian formulation, we compute the motion of particles in the Lagrangian formulation, which is modeled by stochastic differential equations (SDEs). We propose an effective numerical integrator based on a splitting method to solve the corresponding SDEs in which the deterministic subproblem is symplectic preserving while the random subproblem can be viewed as a perturbation. We provide rigorous error analysis for the new numerical integrator using the backward error analysis technique and show that our method outperforms standard Euler-based integrators. Numerical results are presented to demonstrate the accuracy and efficiency of the proposed method for several typical chaotic and stochastic flow problems of physical interest. The existence of residual diffusivity for these flow problems is also investigated.

Key words. diffusion enhancement, chaotic and stochastic flows, effective diffusivity, structure-preserving schemes, stochastic Hamiltonian systems, backward error analysis

AMS subject classifications. 35B27, 60H35, 65P10, 65M75, 76R99

DOI. 10.1137/18M1165219

1. Introduction.

Diffusion enhancement in fluid advection is a fundamental problem to characterize and quantify the large-scale effective diffusion in fluid flows containing complex and turbulent streamlines, which is of great theoretical and practical importance; see [6, 7, 2, 16, 20, 21, 22, 23, 14, 31] and references therein. Its applications can be found in many physical and engineering sciences, including atmosphere/ocean science, chemical engineering, and combustion. In this paper, we study a passive tracer model, which describes particle motion with zero inertia

$$\dot{X}(t) = v(X,t) + \sigma\xi(t), \quad X \in R^d, \tag{1}$$

where X is the position of the particle, $\sigma \geq 0$ is the molecular diffusion coefficient, and $\xi(t) \in R^d$ is a white noise or colored noise. The velocity $v(x,t)$ satisfies either

*Received by the editors January 25, 2018; accepted for publication (in revised form) June 11, 2018; published electronically August 2, 2018.
http://www.siam.org/journals/sinum/56-4/M116521.html
Funding: The research of the first author was partially supported by the Hong Kong PhD Fellowship Scheme. The research of the second author was partially supported by NSF grants DMS-1211179, DMS-1522383. The research of the third author was supported by Hong Kong RGC grants (project 27300616 and 17300817), National Natural Science Foundation of China (project 11601457), Seed Funding Programme for Basic Research (HKU), RAE Improvement Fund from the Faculty of Science (HKU), and the Hung Hing Ying Physical Sciences Research Fund (HKU).
†Department of Mathematics, The University of Hong Kong, Hong Kong 999077, Hong Kong SAR (ariswang@connect.hku.hk).
‡Department of Mathematics, University of California at Irvine, Irvine, CA 92697 (jxin@math.uci.edu).
§Corresponding author. Department of Mathematics, The University of Hong Kong, Hong Kong 999077, Hong Kong SAR (zhangzw@hku.hk).

the Euler or the Navier–Stokes equation. We point out that in practice, $v(x,t)$ can be modeled by a random field which mimics energy spectra of the velocity fields. We set $v(x,t) = \nabla^{\perp}\phi(x,t)$ and the streamline function ϕ satisfies $\phi_t = A\phi + \sqrt{Q}\zeta(x,t)$, which is a random field generated by appropriately choosing operators A and Q and $\zeta(x,t)$ is a space-time white noise independent of $\xi(t)$.

For spatial-temporal periodic velocity fields and random velocity fields with short-range correlations, the homogenization theory [1, 8, 11, 24] says that the long-time large-scale behavior of the particles is governed by a Brownian motion. More precisely, let $D^E \in R^{d\times d}$ denote the effective diffusivity matrix and $X^\epsilon(t) \equiv \epsilon X(t/\epsilon^2)$. Then, $X^\epsilon(t)$ converges in distribution to a Brownian motion $W(t)$ with covariance matrix D^E, i.e., $X^\epsilon(t) \xrightarrow{\mathrm{d}} \sqrt{2D^E}W(t)$. The effective diffusivity matrix D^E can be expressed in terms of particle ensemble average (Lagrangian framework) or integration of solutions to cell problems (Eulerian framework). The dependence of D^E on the velocity field of the problem is highly nontrivial. For a time-independent Taylor–Green velocity field, the authors of [23] proposed a stochastic splitting method and calculated the effective diffusivity in the limit of vanishing molecular diffusion. For random velocity fields with long-range correlations, various forms of anomalous diffusion, such as super-diffusion and sub-diffusion, can be obtained for some exactly solvable models. (See [16] for a review.) However, long-time, large-scale behavior of the particle motion is in general difficult to study analytically.

This motivates us to study numerically the dependence of D^E on complicated incompressible, time-dependent velocity fields in this paper. We are also interested in investigating the existence of residual diffusivity for the passive tracer model (1) for several different velocity fields. The residual diffusivity refers to the nonzero effective diffusivity in the limit of zero molecular diffusion as a result of a fully chaotic mixing of the streamlines. It is expected that the corresponding long-time, large-scale behavior will follow a different law and sensitively depend on the velocity fields. In [15], the authors computed the cell problem of the advection-diffusion type and observed the residual diffusion phenomenon. This approach allows adaptive basis learning for parameterized flows. However, the solutions of the advection-diffusion equation develop sharp gradients as molecular diffusion approaches zero and demand a large amount of computational costs in standard Fourier basis. To overcome this difficulty, we shall adopt the Lagrangian framework and compute an ensemble of particles governed by (1) directly.

In this paper, we shall compute the effective diffusivity of chaotic and stochastic flows using structure-preserving schemes and investigate the existence of residual diffusivity for several prototype velocity fields. First, we propose a new numerical integrator based on a stochastic splitting method to solve the SDEs (1), where the deterministic subproblem is symplectic preserving while the random subproblem can be viewed as a perturbation. Then using the backward error analysis (BEA) [25], we prove that our numerical integrator preserves the invariant measure on torus space (the original space moduled by its space-time period), while the standard Euler-based integrator does not have this property. Thus, our method is capable of computing long-time behaviors of the passive tracer model. Finally, we present several numerical experiments to demonstrate the accuracy and efficiency of the proposed method for several typical chaotic and stochastic flow problems of physical interest.

Though there are several prior works on structure-preserving schemes for ODEs and SDEs, the novelty of our paper is the rigorous theory in the numerical error analysis in computing the effective diffusivity and investigation of nonlinear/random phe-

nomena, such as resonance dependence of residual diffusivity in deterministic chaotic flow on the flow parameters, and lack of it in stochastic flow.

Moreover, the structure-preserving schemes enable us to obtain an improved understanding of the Hamiltonian system with additive noise. Intuitively, when one adds noise to a Hamiltonian system without additional friction, the accumulated thermal energy eventually wipes out detailed dynamics and diffusion becomes dominant on a long-time scale. To investigate the long-time behavior of this new system, one has to make sure that the numerical integration of the dynamics does not artificially inject (or remove) energy into (or from) the system. We find that in this new system, there is still some structure that is nicely preserved, i.e., the invariant measures on the torus. We prove that our structure-preserving scheme follows a first order asymptotic Hamiltonian, which preserves the invariant measures, so that we can accurately compute the effective diffusivity.

The rest of the paper is organized as follows. In section 2, we review the background of the passive tracer model and derivation of the effective diffusivity tensor using multiscale technique. In section 3, we propose our new method for computing the passive tracer model. Error estimate of the proposed method will be discussed in section 4. We use the BEA technique and find that for a class of flows with separable Hamiltonian our method preserves the structure and achieves a linear convergence in computing effective diffusivity. In section 5, we present numerical results to demonstrate the accuracy and efficiency of our method. We also investigate the existence of residual diffusivity for several chaotic and stochastic velocity fields. Concluding remarks are made in section 6.

2. Effective diffusivity and multiscale technique. We first introduce the effective diffusivity for chaotic and stochastic flows. The motion of a particle in a velocity field can be described by the following SDE,

$$\dot{X}(t) = v(X,t) + \sigma\xi(t), \quad X \in R^d, \tag{2}$$

where $\sigma > 0$ is the molecular diffusion, X is the position of the particle, $v(X,t)$ is the Eulerian velocity field at position X, and time t, $\xi(t)$ is a Gaussian white noise with zero mean and correlation function $\langle \xi_i(t)\xi_j(t')\rangle = \delta_{ij}\delta(t-t')$. Here $\langle\cdot\rangle$ denotes ensemble average over all randomness.

Given any initial density $u_0(x)$, the particle $X(t)$ of (2) has a density $u(x,t)$ that satisfies the Fokker–Planck equation,

$$u_t + \nabla\cdot(vu) = D_0\Delta u, \quad u(x,0) = u_0(x), \quad x \in R^d, \tag{3}$$

where $D_0 = \sigma^2/2$ is the diffusion coefficient. When $v(x,t)$ is incompressible (i.e., $\nabla_x \cdot v(x,t) = 0\ \forall t$), deterministic, and space-time periodic in $O(1)$ scale, where we assume the period of $v(x,t)$ is 1 in space and T_{per} in time, the formula for the effective diffusivity tensor is [1, 2]

$$D_{ij}^E = D_0\big(\delta_{ij} + \langle \nabla w_i \cdot \nabla w_j\rangle_p\big), \tag{4}$$

where $w(x,t) \in R^d$ is the periodic solution of the cell problem

$$w_t - v\cdot\nabla w - D_0\triangle w = -v, \quad (x,t) \in \mathbb{T}^d \times [0, T_{per}] \tag{5}$$

and $\langle\cdot\rangle_p$ denotes space-time average over $\mathbb{T}^d \times [0, T_{per}]$. As v is incompressible, solution $w(x,t)$ of the cell problem (5) is unique up to an additive constant by the Fredholm alternative. The correction to D_0 is positive definite in (4).

In practice, the cell problem (5) can be solved using numerical methods, such as spectral methods. In [15], a small set of adaptive basis functions were constructed from fully resolved spectral solutions to reduce the computation cost. However, when D_0 becomes extremely small, the solutions of the advection-diffusion equation (5) develop sharp gradients and demand a large number of Fourier modes to resolve, which makes the Eulerian framework computationally expensive and unstable.

In this paper, we shall investigate the Lagrangian approach to compute the effective diffusivity tensor, which is defined by (equivalent to (4) via homogenization theory)

$$D_{ij}^E = \lim_{t\to\infty} \frac{\Big\langle \big(x_i(t) - x_i(0)\big)\big(x_j(t) - x_j(0)\big)\Big\rangle_r}{2t}, \quad 1 \le i, j \le d, \tag{6}$$

where $X(t) = (x_1(t), \ldots, x_d(t))^T$ is the position of a particle tracer at time t and the average $\langle\cdot\rangle_r$ is taken over an ensemble of test particles. If the above limit exists, that means the transport of the particle is a standard diffusion process, at least on a long-time scale. This is the typical situation, i.e., the spreading of the particle $\langle(x_i(t) - x_i(0))(x_j(t) - x_j(0))\rangle_r$ grows linearly with respect to time t, for example, when the velocity field is given by the Taylor–Green velocity field [23]. However, there are also cases showing that the spreading of particles does not grow linearly with time but has a power law t^γ, where $\gamma > 1$ and $\gamma < 1$ correspond to superdiffusive and subdiffusive behaviors, respectively [2, 16].

The major difficulty in solving (2) comes from the fact that the computational time should be long enough to approach the diffusion time scale. To address this challenge, we shall develop robust numerical integrators, which are structure-preserving and accurate for long-time integration. In addition, we shall investigate the relationship between several typical time-dependent velocity fields $v(x, t)$ (including chaotic flows and stochastic flows) and the corresponding effective diffusivity in this paper.

3. New stochastic integrators. In this section, we construct the new stochastic integrators for the passive tracer model, which is based on the operator splitting methods [27, 17]. We consider the following two-dimensional model problems to illustrate the main idea,

$$\begin{cases} dx_1 = v_1(x_1, x_2, t)dt + \sigma_1 dW_1, & x_1(0) = x_{10}, \\ dx_2 = v_2(x_1, x_2, t)dt + \sigma_2 dW_2, & x_2(0) = x_{20}. \end{cases} \tag{7}$$

Furthermore, we assume that there exists a Hamiltonian function $H(x_1, x_2, t)$ such that

$$v_1(x_1, x_2, t) = -\frac{\partial H(x_1, x_2, t)}{\partial x_2}, \quad v_2(x_1, x_2, t) = \frac{\partial H(x_1, x_2, t)}{\partial x_1}. \tag{8}$$

In this paper we assume that the Hamiltonian $H(x_1, x_2, t)$ is sufficiently smooth and that first order derivatives of $v_i(x_1, x_2, t)$, $i = 1, 2$ are bounded. These conditions are necessary to guarantee the existence and uniqueness of solutions of the SDE (7); see [19]. Moreover, the boundedness of some higher order derivatives of $v_i(x_1, x_2, t)$ is required when we prove the convergence analysis in section 4.

We first formally rewrite the particle tracer model (7) into an abstract form $dX = \mathcal{L}X$, where $X = (x_1, x_2)^T$. We then split the operator $\mathcal{L}$ into two operators $\mathcal{L}_i$,

$i = 1, 2$, where

$$\mathcal{L}_1 : \quad dx_1 = v_1(x_1, x_2, t)dt, \quad dx_2 = v_2(x_1, x_2, t)dt, \tag{9}$$

$$\mathcal{L}_2 : \quad dx_1 = \sigma_1 dW_1, \qquad dx_2 = \sigma_2 dW_2, \tag{10}$$

corresponding to the deterministic part and the stochastic part, respectively. Finally, we apply the operator splitting method [17] to approximate the integrator $\varphi(\tau) = exp(\tau(\mathcal{L}_1 + \mathcal{L}_2))$ generated from (7). The operator splitting methods have been successfully applied to various problems, although there is limited work on solving SDEs and SPDEs. We refer to [18, 3, 28, 30] for recent works on Hamiltonian systems with additive noise.

We approximate the integrator $\varphi(\tau)$ by the Lie–Trotter splitting method and get

$$\varphi(\tau) = exp(\tau(\mathcal{L}_1 + \mathcal{L}_2)) \approx exp(\tau\mathcal{L}_1)exp(\tau\mathcal{L}_2). \tag{11}$$

Now we discuss how to discretize the numerical integrator (11). From time $t = t_k$ to time $t = t_{k+1}$, where $t_{k+1} = t_k + \tau$, $t_0 = 0$, assuming the solution $(x_1^k, x_2^k)^T \equiv (x_1(t_k), x_2(t_k))^T$ is given, one solves the subproblems corresponding to $\mathcal{L}_1$ and $\mathcal{L}_2$ in a small time step τ to obtain $(x_1^{k+1}, x_2^{k+1})^T$. In our numerical method, we discretize the operator $\mathcal{L}_1$ by numerical schemes that preserve symplectic structure and the operator $\mathcal{L}_2$ by the Euler–Maruyama scheme [19], so we obtain the new stochastic integrators for (7) as follows,

$$\begin{cases} x_1^* = x_1^k + \tau v_1\big(\alpha x_1^* + (1-\alpha)x_1^k, (1-\alpha)x_2^* + \alpha x_2^k, t_k + \beta\tau\big), \\ x_2^* = x_2^k + \tau v_2\big(\alpha x_1^* + (1-\alpha)x_1^k, (1-\alpha)x_2^* + \alpha x_2^k, t_k + \beta\tau\big), \end{cases} \tag{12}$$

where the parameters $\alpha, \beta \in [0, 1]$ and

$$\begin{cases} x_1^{k+1} = x_1^* + \sigma_1 \Delta_k W_1(\tau), \\ x_2^{k+1} = x_2^* + \sigma_2 \Delta_k W_2(\tau) \end{cases} \tag{13}$$

with $\Delta_k W_i(\tau) = W_i(t_k + \tau) - W_i(t_k)$, $i = 1, 2$. In practice, each $\Delta_k W_i(\tau)$ is an independent random variable of the form $\sqrt{\tau}\mathcal{N}(0, 1)$.

The symplectic-preserving schemes (12) are implicit in general. Compared with explicit schemes, however, they allow us to choose a relatively larger time step to compute. In practice, we find that few steps of Newton iterations are enough to maintain accurate results. Therefore, the computational cost is controllable. To design an adaptive time-stepping method for (7) is an interesting issue, which will be studied in our future work.

We should point out that when the Hamiltonian function is separable, which is true in many physics problems, we can choose $\alpha = 0$ or $\alpha = 1$ so that one component of (12) becomes explicit. Investigations for the problems with nonseparable Hamiltonian can be more difficult, which will be our future work. The interested reader is referred to [28] for a recent work on the explicit symplectic approximation of nonseparable Hamiltonians.

In general, the second order Strang splitting [27] is more frequently adopted in application, for which the integrator $\varphi(\tau)$ is approximated by

$$\varphi(\tau) = exp(\tau(\mathcal{L}_1 + \mathcal{L}_2)) \approx exp\left(\frac{\tau}{2}\mathcal{L}_2\right) exp\left(\tau\mathcal{L}_1\right) exp\left(\frac{\tau}{2}\mathcal{L}_2\right). \tag{14}$$

In fact, the only difference between the Strang splitting method and the Lie–Trotter splitting method is that the first and last steps are half of the normal step τ. Thus a more accurate method can be implemented in a very simple way. We skip the details in implementing the Strang splitting scheme here as it is straightforward.

We remark that our new stochastic integrators provide an efficient way to investigate the residual diffusivity, because we do not need to solve the advection-diffusion equation (5), which becomes extremely challenging when D_0 is small. Most importantly, symplectic-preserving schemes provide a robust and accurate numerical integrator for long-time integrations. We shall theoretically and numerically study their performance over existing numerical integrators, such as Euler schemes, in sections 4 and 5.

4. Convergence analysis. In this section, we shall provide some convergence results. We prove that a linear growth of the global error can be obtained if we apply our numerical methods to compute a class of flows with a separable Hamiltonian. In addition, we shall estimate the numerical error in computing the effective diffusivity. Our analysis is based on the BEA technique [25], which is a powerful tool to study the long-time behaviors of numerical integrators.

4.1. Weak Taylor expansion. In our derivation, we use (p, q) to denote the position of a particle interchangeably with (x_1, x_2). In addition, we assume $\sigma_1 = \sigma_2 = \sigma$. Thus, the Hamiltonian system defined by (7) is rewritten as

$$\begin{cases} dp = -H_q dt + \sigma dW_1, \\ dq = H_p dt + \sigma dW_2, \end{cases} \tag{15}$$

where $H \equiv H(p, q, t)$ is the Hamiltonian and dW_i, $i = 1, 2$ are two independent Brownian motion processes. We assume the Hamiltonian H has a separable form [10]

$$H(p, q, t) = F(p, t) + G(q, t) \tag{16}$$

with $g \equiv H_q = g(q, t)$ and $f \equiv H_p = f(q, t)$.

Remark 4.1. The separable Hamiltonian is quite a natural assumption and has many applications in physical and engineering sciences. For instance, $H(p, q) = \frac{1}{2}p^T p + U(q)$, where the first term is the kinetic energy and the second one is the potential energy.

One natural way to study the expectations of the paths for the SDE given by (15) is to consider its associated backward Kolmogorov equation [26]. Specifically, we associate the SDE with a partial differential operator $\mathcal{L}_0$, which is called the generator of the SDE, also known as the flow operator. For the Hamiltonian system (15), the corresponding backward Kolmogorov equation is given by

$$\begin{cases} \frac{\partial}{\partial t}\phi = \mathcal{L}_0 \phi, \\ \phi(x, 0) = \phi_0(x), \end{cases} \tag{17}$$

where the operator $\mathcal{L}_0$ is given by

$$\mathcal{L}_0 = -g\partial_p + f\partial_q + \frac{1}{2}\sigma^2\partial_p^2 + \frac{1}{2}\sigma^2\partial_q^2. \tag{18}$$

A probabilistic interpretation of (17) is that given initial data $\phi_0(x)$, the solution of (17), $\phi(x, t)$ satisfies $\phi(x, t) = E(\phi_0(X_t)|X_0 = x)$, where $X_t = (p(t), q(t))$ is the

solution to (15). We integrate (17) from $t = 0$ to $t = \Delta t$ and obtain

$$\phi(x, \Delta t) = \phi(x, 0) + \mathcal{L}_0 \int_0^{\Delta t} \phi(x, s) ds. \tag{19}$$

Under certain regularity assumptions on the drift terms g and f, the solution $\phi(x, t)$ is $N+1$ time differentiable with respect to time t. Thus, when Δt is sufficiently small, we have the Taylor expansion

$$\phi(x, s) = \phi(x, 0) + s\frac{\partial}{\partial s}\phi(x, 0) + \cdots + \frac{s^N}{N!}\frac{\partial^N}{\partial s^N}\phi(x, 0) + R_N(x, s), \quad s \in (0, \Delta t), \tag{20}$$

where $R_N(x, s)$ is the remainder term in the Taylor expansion and $R_N(x, s) \to 0$ as $\Delta t \to 0$ $\forall x$. This local Taylor expansion result plays an important role in our BEA. We substitute the Taylor expansion (20) into (19) and get

$$\phi(x, \Delta t) = \phi(x, 0) + \Delta t \mathcal{L}_0 \phi(x, 0) + \sum_{k=1}^{N} \frac{\Delta t^{k+1}}{(k+1)!} \mathcal{L}_0 \frac{\partial^k}{\partial s^k}\phi(x, 0) + O(\Delta t^{N+2}). \tag{21}$$

Recalling that $\phi(x, 0) = \phi_0(x)$ and $\frac{\partial^k}{\partial s^k}\phi(x, 0) = \mathcal{L}_0^k \phi_0(x)$, we finally obtain

$$\phi(x, \Delta t) = \phi_0(x) + \sum_{k=0}^{N} \frac{\Delta t^{k+1}}{(k+1)!} \mathcal{L}_0^{k+1} \phi_0(x) + O(\Delta t^{N+2}). \tag{22}$$

The operator $\mathcal{L}_0^{k+1}$ can be computed systematically. For instance, $\mathcal{L}_0$ defined in (18) has 4 terms, then $\mathcal{L}_0^2$ should have at most $4^2 = 16$ terms. In this paper, we find that the first order modified equation has already indicated the advantage of the structure-preserving scheme.

Remark 4.2. Equation (22) provides a general framework for us to analyze the truncation error by numerical methods. Namely, the numerical flow $\phi^{num}(x, \Delta t) = E[\phi_0(X_{\Delta t}^{num,k})|X_0 = x]$ generated by a kth order weak method should satisfy (22) up to terms of order $O(\Delta t^k)$.

4.2. First order modified equation. In this section, we shall analyze the numerical errors obtained by our symplectic splitting scheme and Euler–Maruyama scheme [12], respectively. We find that the solution obtained by the symplectic splitting scheme follows an asymptotic Hamiltonian while the solution obtained by the Euler–Maruyama scheme does not. With our new method, we can achieve a linear growth (instead of an exponential growth) of the global error when we compute effective diffusivity.

After numerical discretization, we find the following expansion using a first order weak method at $t = \Delta t$,

$$\phi^{num}(x, \Delta t) = \phi_0(x) + \Delta t \mathcal{L}_0 \phi_0(x) + \Delta t^2 \mathcal{A}_1 \phi_0(x) + O(\Delta t^3), \tag{23}$$

where $\mathcal{A}_1$ is a partial differential operator acting on $\phi_0(x)$ that depends on the choice of the numerical method used to solve (15). If we choose a convergent method to discretize the operator $\mathcal{L}_0$ in (23) and (21), then the local truncation error is $O(\Delta t^2)$ and the numerical scheme is of weak order one. We refer to [12] for the definition and discussion of the weak convergence and strong convergence.

Specifically, let $X^{num}(\Delta t) = (p(\Delta t), q(\Delta t))$ denote the numerical solution obtained by one specific choice of the numerical method in solving (15). For instance, if we choose the symplectic splitting method stated in (12), (13) and set $\alpha = 0$ and $\beta = \frac{1}{2}$, we get

$$\begin{cases} p(\Delta t) = p_0 - \Delta t g(q_0, \frac{\Delta t}{2}) + \sigma \Delta W_1, \\ q(\Delta t) = q_0 + \Delta t f(p_0 - \Delta t g(\frac{\Delta t}{2}, q_0), \frac{\Delta t}{2}) + \sigma \Delta W_2. \end{cases} \tag{24}$$

Now ΔW_1, ΔW_2 are two independent random variables of the form $\sqrt{\Delta t}\mathcal{N}(0,1)$. To get $\mathcal{A}_1$, we only need to expand $E(\phi_0(p(\Delta t), q(\Delta t)))$ around point $\phi_0(p_0, q_0)$ with respect to the time variable Δt. Since we are dealing with a separable Hamiltonian H, the operator splitting scheme helps us obtain a straightforward adaptive interpolation of (24) for $t \in [0, \Delta t]$, saying X_t^{num}. We then have the form [32]

$$\phi^{num}(x,t) = E[\phi_0(X_t^{num})|X_0 = (p_0, q_0)] \tag{25}$$

$$= \phi_0(x) + \Delta t \mathcal{L}_0 \phi_0(x) + \Delta t^2 \mathcal{A}_1 \phi_0(x) + O(\Delta t^3). \tag{26}$$

In the BEA [25], we aim to find the generator $\mathcal{L}^{num}$ of this process and the associated backward Kolmogorov equation,

$$\begin{cases} \frac{\partial}{\partial t}\phi^{num} = \mathcal{L}^{num}\phi^{num}, \\ \phi^{num}(x,0) = \phi_0(x). \end{cases} \tag{27}$$

We now denote the generator of this modified equation in an asymptotic form in terms of Δt,

$$\mathcal{L}^{num} \equiv \mathcal{L}_0 + \Delta t \mathcal{L}_1 + \Delta t^2 \mathcal{L}_2 + \cdots. \tag{28}$$

Recall that the operator $\mathcal{L}_0$ is defined in (18) and the definition of operators $\mathcal{L}_i$, $i \geq 1$, depends on the choice of the numerical method in solving (15). We substitute (28) into (22) then compare with (26) and get

$$\mathcal{L}_1 = \mathcal{A}_1 - \frac{1}{2}\mathcal{L}_0^2. \tag{29}$$

Now let us denote the truncated generator by

$$\mathcal{L}^{\Delta t,k} \equiv \mathcal{L}_0 + \Delta t \mathcal{L}_1 + \cdots + \Delta t^k \mathcal{L}_k \tag{30}$$

and define the corresponding modified flow (if it exists) as

$$\begin{cases} \frac{\partial}{\partial t}\phi^{\Delta t} = \mathcal{L}^{\Delta t,k}\phi^{\Delta t}, \\ \phi^{\Delta t}(x,0) = \phi_0(x). \end{cases} \tag{31}$$

Inspired by the weak convergence proof in [12], we shall focus on estimating the upper bound of the uniform numerical error for the perturbed flows.

LEMMA 4.1. *Let ϕ^{num} and $\phi^{\Delta t}$ be defined in* (27) *and* (31)*, respectively. We assume that $\phi_0 \in \mathcal{C}^\infty$ and its Ito–Taylor expansion coefficients in the hierarchy set $\Gamma_{k+1} \bigcup B(\Gamma_{k+1})$ are Lipschitz and have at most linear growth. If the solution to the first order modified flow $\phi^{\Delta t}$ converges to ϕ as $\Delta t \to 0$, then we have the following error estimate:*

$$||\phi^{num}(x,t) - \phi^{\Delta t}(x,t)|| \leq C(T)\Delta t^{k+1}. \tag{32}$$

Proof. Equation (23) shows that the operator $L^{\Delta t}$ approximates the operator $L^{\Delta t,k}$ locally in the time interval $[0, \Delta t]$ with the truncation error $O(\Delta t^{k+2})$. This implies that $X_t^{\Delta t}$ is a $k+1$th order weak approximation to the SDE related to $X_t^{\Delta t,k}$ locally, i.e.,

(33)
$$\phi_0(X_{\Delta t}^{num}) - \phi_0(X_{\Delta t}^{\Delta t,k}) = \phi_0(X_0^{num}) - \phi_0(X_0^{\Delta t,k}) + \sum_{\alpha \in B(\Gamma_{k+1})} I_\alpha[\phi_{0,\alpha}(X_{(\cdot)}^{\Delta t,k})]_{0,\Delta t}.$$

Here we refer to Chapter 5.5 in [12] for a more detailed definition of multi-index stochastic Ito integration notation I_α. Proposition 5.11.1 in [12] gives an estimate for the I_α,

$$\left| E \sum_{\alpha \in B(\Gamma_{k+1})} I_\alpha[\phi_{0,\alpha}(X_{(\cdot)}^{\Delta t,k})]_{0,\Delta t} \right| \le C(L^{\Delta t,k})\Delta t^{k+2}. \tag{34}$$

Since the operator $L^{\Delta t,k}$ approximates L_0 and $\lim_{\Delta t \to 0} C(L^{\Delta t,k}) = C(L)$, combining with Lipschitz and linear growth condition, the final weak convergence order should be $C(T)\Delta t^{k+1}$ when Δt is small enough. ∎

Remark 4.3. Figure 1 shows the general procedure of our convergence analysis. Our goal is to develop efficient numerical methods so that we can reduce the numerical error in computing effective diffusivity $|D^E - D^{E,num}|$, which is the dashed line on the left. Recall that D^E is the exact effective diffusivity defined by the (6) and $D^{E,num}$ is the numerical result obtained using our method. It is however difficult to estimate the error $|D^E - D^{E,num}|$. The BEA (shown in the middle row) provides a general framework that allows us to calculate modified equations induced by different numerical methods and estimate the errors between the numerical solutions (shown in the upper row) and the analytic ones (shown in the bottom row). This framework clearly reveals the main sources of error (i.e., $|D^{E,\Delta t} - D^E|$). The notation (e.g., $D^{E,\Delta t}$, $X_t^{\Delta t,k}(or\ X_t^{\Delta t})$, $\mathcal{L}^{\Delta t,k} : \phi^{\Delta t}$) is introduced from the BEA and is frequently used in section 4.

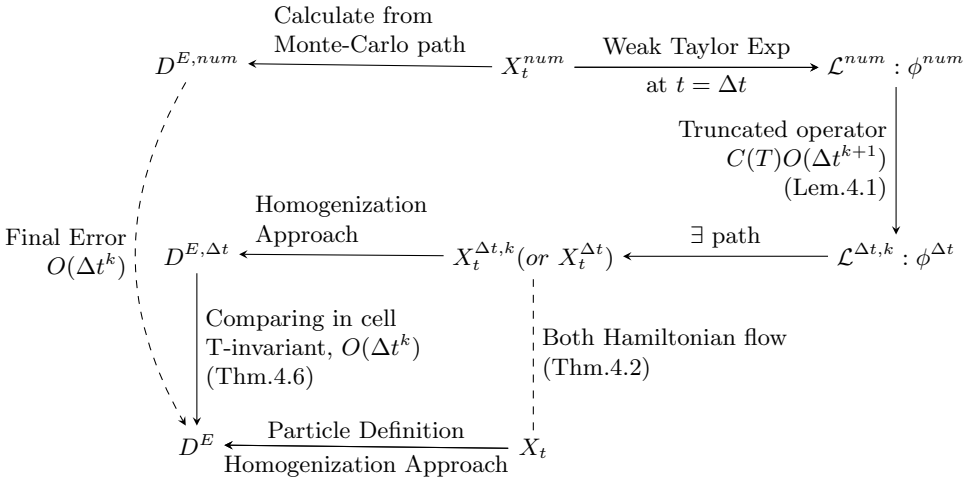

FIG. 1. *Illustration of BEA for kth order weak scheme.*

The foregoing derivation shows that modified flows allow us to approximate the interpolation of a numerical solution with a higher order accuracy. Hence the modified flows dominate the error in the numerical result. Now we intend to study the behavior of the modified flows.

THEOREM 4.2. *For the stochastic differential equation system* (15) *with a time-independent and separable Hamiltonian* $H(p,q)$ (16)*, the numerical solution obtained using the symplectic splitting scheme follows an asymptotic Hamiltonian* $H^{\Delta t}(p,q)$*, or equivalently, the first order modified equation (density function) of the solution is divergence-free. The invariant measure on torus (defined by* $\mathbb{R}^d/\mathbb{Z}^d$*, when period is* 1*) remains uniform, which is also known as the Haar measure, while the numerical solution obtained using the Euler–Maruyama scheme does not have these properties.*

Proof. We shall compare the generators of modified equations obtained by using the symplectic splitting scheme and Euler–Maruyama scheme, respectively. More specifically, we compare the operator $\mathcal{L}_1$ in (28) obtained from different methods. In the symplectic splitting scheme, we compute the weak Taylor expansion at time $t = \Delta t$ and get

$$\begin{aligned}(35)\quad \mathcal{L}_1\phi &= \left(\mathcal{A}_1 - \frac{1}{2}\mathcal{L}_0^2\right)\phi \\ &= \left(\frac{1}{2}fg' + \frac{\sigma^2}{4}g''\right)\phi_p + \left(-\frac{1}{2}f'g - \frac{\sigma^2}{4}f''\right)\phi_q + \left(-\frac{\sigma^2}{2}f' + \frac{\sigma^2}{2}g'\right)\phi_{pq}.\end{aligned}$$

Hence, the modified flow of $X^{\Delta t,k}$ can be written as

$$(36)\qquad \begin{cases} dp = (-g + (\frac{1}{2}fg' + \frac{\sigma^2}{4}g'')\Delta t)dt + \sigma dW_1 + \Delta t\frac{\sigma}{2}g'dW_2, \\ dq = (f - (\frac{1}{2}f'g + \frac{\sigma^2}{4}f'')\Delta t)dt + \sigma dW_2 - \Delta t\frac{\sigma}{2}f'dW_1. \end{cases}$$

Similarly, in the Euler–Maruyama scheme, we get that

$$\begin{aligned}(37)\quad \mathcal{L}_1\phi &= \left(\mathcal{A}_1 - \frac{1}{2}\mathcal{L}_0^2\right)\phi \\ &= \left(\frac{1}{2}fg' + \frac{\sigma^2}{4}g''\right)\phi_p + \left(\frac{1}{2}f'g - \frac{\sigma^2}{4}f''\right)\phi_q + \left(-\frac{\sigma^2}{2}f' + \frac{\sigma^2}{2}g'\right)\phi_{pq}.\end{aligned}$$

And the associated modified flow can be written as

$$(38)\qquad \begin{cases} dp = (-g + (\frac{1}{2}fg' + \frac{\sigma^2}{4}g'')\Delta t)dt + \sigma dW_1 + \Delta t\frac{\sigma}{2}g'dW_2, \\ dq = (f - (-\frac{1}{2}f'g + \frac{\sigma^2}{4}f'')\Delta t)dt + \sigma dW_2 - \Delta t\frac{\sigma}{2}f'dW_1. \end{cases}$$

Comparing the results from (36) and (38), we can easily find that (36) follows an asymptotic Hamiltonian,

$$(39)\qquad H^{\Delta t} \equiv H - \Delta t\left(\frac{1}{2}fg + \frac{\sigma^2}{4}(f' + g')\right),$$

where we mainly focus on the first order approximation so we remove the high order terms. In contrast, the flow (38) obtained from the Euler–Maruyama scheme does not have this structure. Furthermore, we introduce notation v_1 and d_1 to denote extra terms in the modified flow (36), which are defined as

$$(40)\qquad v_1 = \begin{pmatrix} \frac{1}{2}fg' + \frac{\sigma^2}{4}g'' \\ -\frac{1}{2}f'g - \frac{\sigma^2}{4}f'' \end{pmatrix}, \quad \text{and} \quad d_1 = \begin{pmatrix} 0 & \frac{1}{2}g' \\ -\frac{1}{2}f' & 0 \end{pmatrix}.$$

Since our numerical method solves an SDE determined by a modified flow (36), the density function of particles $u(x,t)$ obtained using our method satisfies a modified Fokker–Planck equation given by

$$u_t = -(v + \Delta t v_1)\nabla u + D_0 \nabla\nabla : (I_d + \Delta t D_1)u, \tag{41}$$

where I_d is a d-dimensional identity matrix and

$$D_1 = \frac{1}{\Delta t}\big((I_d + \Delta t d_1)(I_d + \Delta t d_1)^T - I_d\big) = \begin{pmatrix} \frac{\Delta t}{4}(g')^2 & \frac{1}{2}(g' - f') \\ \frac{1}{2}(g' - f') & \frac{\Delta t}{4}(f')^2 \end{pmatrix}.$$

We have used the condition $\nabla \cdot v_1 = 0$ to get $\nabla\big((v + \Delta t v_1)u\big) = (v + \Delta t v_1)\nabla u$. The inner product between matrices is denoted by $A : B = tr(A^T B) = \sum_{i,j} a_{ij} b_{ij}$. It follows that $\nabla\nabla : I = \Delta$ and $\nabla\nabla : D_1$ are defined accordingly. Finally, we can find that (41) admits trivial invariant measure $u(x,t) \equiv 1$. ∎

We can repeat a similar calculation and generalize the results of Theorem 4.2 to a general time-dependant and separable Hamiltonian. Therefore, we obtain the results as follows.

COROLLARY 4.3. *For the stochastic differential equation system* (15) *with a time-dependent and separable Hamiltonian* H (16)*, the numerical solution obtained using the symplectic splitting scheme follows an asymptotic Hamiltonian* $H^{\Delta t}$*, or equivalently, the first order modified equation (density function) of the solution is divergence-free. The invariant measure on torus (defined by* $\mathbb{R}^d/\mathbb{Z}^d$*, when period is* 1*) remains uniform, which is also known as the Haar measure, while the numerical solution obtained using the Euler–Maruyama scheme does not have these properties.*

Proof. We repeat the same computation as we did in proving the Theorem 4.2. In the symplectic splitting scheme, we find that the corresponding modified flow can be written as

$$\begin{cases} dp = \big(-g + (\frac{1}{2}fg' + \frac{\sigma^2}{4}g'' + \frac{1}{2}g_t)\Delta t\big)dt + \sigma dW_1 + \Delta t\frac{\sigma}{2}g' dW_2, \\ dq = \big(f - (\frac{1}{2}f'g + \frac{\sigma^2}{4}f'' + \frac{1}{2}f_t)\Delta t\big)dt + \sigma dW_2 - \Delta t\frac{\sigma}{2}f' dW_1. \end{cases} \tag{42}$$

The rest part of the proof is similar to Theorem 4.2 so we skip the details. ∎

Before we end this subsection, we use an example to demonstrate our main idea. We consider the flow driven by the Taylor–Green velocity field,

$$\begin{cases} dp = -\cos(q)\sin(p)dt + \sigma dW_1, \\ dq = \sin(q)\cos(p)dt + \sigma dW_2. \end{cases} \tag{43}$$

By introducing two variables $P = p + q$ and $Q = p - q$, we know the dynamic system (43) possesses a separable Hamiltonian $H = -\cos P - \cos Q$ and the system can be expressed as

$$\begin{cases} dP = -\sin Q dt + \sqrt{2}\sigma d\eta_1, \\ dQ = \sin P dt + \sqrt{2}\sigma d\eta_2, \end{cases} \tag{44}$$

where η_1 and η_2 are two independent Brownian motions that are linear combinations of W_1 and W_2. With simple calculations according to (36) and (39), we get

$$\begin{cases} dP = -\frac{\partial H^{\Delta t}}{\partial Q}dt + \sqrt{2}\sigma d\eta_1 + \Delta t\frac{\sigma}{\sqrt{2}}\cos Q d\eta_2, \\ dQ = \frac{\partial H^{\Delta t}}{\partial P}dt + \sqrt{2}\sigma d\eta_2 + \Delta t\frac{\sigma}{\sqrt{2}}\cos P d\eta_1, \end{cases} \tag{45}$$

and

$$H^{\Delta t} = H - \Delta t\left(\frac{1}{2}\sin P \sin Q + \frac{\sigma^2}{2}(\cos P + \cos Q)\right). \tag{46}$$

Up to now, the new integrator (7) is shown to preserve the structure of original Hamiltonian system (15) asymptotically at $O(\Delta t)$. In the next subsection, we shall show that the new integrator leads to an efficient method in computing effective diffusivity due to its structure-preserving property.

4.3. Error analysis in computing effective diffusivity. Notice that in (6) only distribution of the process is needed, so the Eulerian framework is sufficient to get an error estimate. For the sake of comparison, we rewrite the effective diffusivity formula (4) for (7) as

$$D^E = D_0\big\langle (I_d + \nabla w)(I_d + \nabla w)^T\big\rangle_p, \tag{47}$$

where $D_0 = \sigma^2/2$ and cell problem w satisfies

$$w_t - (v \cdot \nabla w) - D_0 \Delta w = -v \tag{48}$$

with the velocity filed $v = (-g, f)^T$. To study the effective diffusivity defined in (41), we turn to [1, section 3.10], where an exact formula for D^E in a nonconstant diffusion case is provided. Let $w^{\Delta t} \equiv w^{\Delta t}(t, x)$ denote the periodic solution of the modified cell problem that is corresponding to the modified Fokker–Planck equation (41), i.e., $w^{\Delta t}$ satisfies the following equation:

$$w_t^{\Delta t} = (v + \Delta t v_1) \cdot \nabla w^{\Delta t} + D_0 \nabla\nabla : (I + \Delta t D_1) w^{\Delta t} - (v + \Delta t v_1). \tag{49}$$

We introduce two operators defined as $\mathcal{P}_0 w^{\Delta t} \equiv v\nabla w^{\Delta t} + D_0 \Delta w^{\Delta t}$ and $\mathcal{P}_1 w^{\Delta t} \equiv v_1 \nabla w^{\Delta t} + D_0 \nabla\nabla : D_1 w^{\Delta t}$ so we simplify (49) as

$$w_t^{\Delta t} = (\mathcal{P}_0 + \Delta t \mathcal{P}_1) w^{\Delta t} - (v + \Delta t v_1). \tag{50}$$

Now by Theorem 4.2 and Corollary 4.3, we know that (36) admits a trivial invariant measure, so the formula for the effective diffusivity tensor reads

$$D^{E,\Delta t} = D_0\Big\langle (I_d + \nabla w^{\Delta t})(I_d + \Delta t D_1)(I_d + \nabla w^{\Delta t})^T\Big\rangle_p. \tag{51}$$

The modified cell problem (49) and the corresponding effective diffusivity tensor (51) enable us to analyze the numerical error in our new method.

LEMMA 4.4. *Equation* (49) *has a unique solution if the condition* $\int_{U_T} w^{\Delta t} dx dt = 0$ *holds, where* $U_T = [0, T] \times U$ *is the space-time domain for the periodic function* w.

Proof. We first notice that when $\Delta t \ll D_0$, the operator $(\mathcal{P}_0 + \Delta t \mathcal{P}_1)$ is uniformly elliptic. The space average of the source term $-(v + \Delta t v_1)$ vanishes. By the Fredholm alternative, (50) has nontrivial solutions if $-(v + \Delta t v_1) \not\equiv 0$. Then, using the maximum principle, we get the conclusion that the solution $w^{\Delta t}$ to (49) is unique if the condition $\int_{U_T} w^{\Delta t} dx dt = 0$ is satisfied. ∎

Now we derive a regularity estimate in this Poincaré map problem (49).

THEOREM 4.5. *Suppose $w = w(t,x)$ is a space-time periodic solution over the domain $U_T = [0,T] \times U$, which satisfies*

$$w_t - (v \cdot \nabla w) - D : \nabla\nabla w = S, \ (t,x) \in U_T = [0,T] \times U, \tag{52}$$

where $\nabla \cdot v = 0$, D is a symmetric positive-definite matrix and its eigenvalues have positive lower and upper bounds, i.e., there exist $D_+ > D_- > 0$ so that eigenvalues of D are in $[D_-, D_+]$ $\forall (x,t)$, and $S = S(t,x)$ is the source term, which vanishes in average at any time t. Then, we have the regularity estimate for w as $|\nabla w|_{L_2(U_T)} \leq C|S|_{L_2(U_T)}$, where the constant C depends only on the length of the physical domain U and the eigenvalues of D.

Proof. We multiply (52) by w^T, integrate over U, and get

$$\int_U (w^T w_t - w^T v \nabla w - w^T D : \nabla\nabla w) dx = \int_U w^T S dx. \tag{53}$$

We notice that

$$\int_U w^T w_t dx = \frac{d}{dt} \int_U |w|^2 dx,$$
$$\int_U w^T v \nabla w dx = -\int_U w^T v \nabla w dx = 0,$$
$$\int_U -w^T D : \nabla\nabla w dx = \int_U \nabla w^T D \nabla w dx,$$

where we have used the condition $\nabla \cdot v = 0$. Then, we integrate (53) over the time period $[0,T]$ and the periodic condition of w implies

$$\int_{U_T} \nabla w^T D \nabla w dx = \int_{U_T} w^T S dx dt. \tag{54}$$

Let $\bar{w}(t)$ denote the space average of w at time t. Since S vanishes in space average at any time t, we have

$$\int_{U_T} \bar{w}^T S dx dt = 0. \tag{55}$$

In addition, we get the equality

$$\left(\int_{U_T} \nabla w^T D \nabla w dx \right)^2 = \left(\int_{U_T} (w^T - \bar{w}^T) S dx dt \right)^2. \tag{56}$$

Applying the Poincaré inequality on the right-hand side and the Cauchy–Schwartz inequality on the left, we obtain the estimate

$$\int_{U_T} \nabla w^T D \nabla w dx \geq D_- \int_{U_T} |\nabla w|^2 dx dt \geq \int_{[0,T]} C_U \int_U |w - \bar{w}|^2 dx dt = \int_{U_T} |w - \bar{w}|^2 dx dt, \tag{57}$$

$$\left(\int_{U_T} (w^T - \bar{w}^T) S dx dt \right)^2 \leq \int_{U_T} |S|^2 dx dt \int_{U_T} |w - \bar{w}|^2 dx dt. \tag{58}$$

Finally combining the inequalities (57) and (58), we get the regularity estimate in L_2 norm.

$$|\nabla w|_{L_2(U_T)} \leq \frac{C(U)}{D_-} |S|_{L_2(U_T)}. \tag{59}$$

∎

Given the regularity estimate derived in Theorem 4.5, we can easily get an estimate for the error between solutions to (48) and (49). We summarize the main result into the following theorem.

THEOREM 4.6. *Let $w(x,t)$ and $w^{\Delta t}(x,t)$ be the solution to the* (48) *and* (49)*, respectively. We have the estimate $|\nabla w - \nabla w^{\Delta t}|_{L_2(U_T)} \le C_U \frac{\Delta t}{D_0} |S_e|_{L_2(U_T)}$, where $S_e = \mathcal{P}_1 w^{\Delta t} - v_1$ is the source term.*

Proof. Let $e \equiv e(x,t) = w(x,t) - w^{\Delta t}(x,t)$ denote the error. One can easily find that $e(x,t)$ is a space-time periodic function over $U_T = [0,T] \times U$ and satisfies the equation

$$e_t - (v \cdot \nabla e) - D_0 \Delta e = (\Delta t) S_e. \tag{60}$$

where the source term $S_e = \mathcal{P}_1 w^{\Delta t} - v_1$. So we directly apply the regularity estimate obtained in Theorem 4.5 for the (60) and obtain

$$|\nabla e|_{L_2(U^T)} \le C(U) \frac{\Delta t}{D_0} |\mathcal{P}_1 w^{\Delta t} - v_1|_{L_2(U^T)}. \tag{61}$$

Again when $\Delta t \ll D_0$, the operator $\frac{\partial}{\partial t} + (\mathcal{P}_0 + \Delta t \mathcal{P}_1)$ is uniformly parabolic and the diffusion coefficients $D = D_0 + \Delta t D_1$ is positive and uniformly bounded below (i.e., $D \to D_0$) for Δt small enough. By a regularity estimate of the parabolic equation (see [5]), we can get that $w^{\Delta t}$, $\nabla w^{\Delta t}$, and $\nabla\nabla : w^{\Delta t}$ are uniformly bounded in $L_2(U_T)$ for Δt small enough. Hence, we obtain

$$|\mathcal{P}_1 w^{\Delta t} - v_1|_{L_2(U_T)} = |(v_1 \nabla + D_0 \nabla\nabla : D_1) w^{\Delta t} - v_1|_{L_2(U_T)} \le C, \tag{62}$$

where the constant C is independent of Δt. ∎

Remark 4.4. From the estimate (61), we know that a proper setting for the time step in calculating effective diffusivity should be

$$\Delta t \sim D_0 = \frac{\sigma^2}{2}. \tag{63}$$

Finally, based on the error estimate for the solutions to the cell problems (48) and (49), we are able to get the error analysis for the effective diffusivity in our method.

THEOREM 4.7. *Let D^E and $D^{E,\Delta t}$ denote the effective diffusivity tensor computed by* (47) *and* (51)*. Then, the error of the effective diffusivity tensor can be bounded by*

$$|D^{E,\Delta t} - D^E| \le C \Delta t, \tag{64}$$

where the constant C does not depend on time T.

Proof. Recall (51), $D^{E,\Delta t} = D_0 \Big\langle (I_d + \nabla w^{\Delta t})(I_d + \Delta t D_1)(I_d + \nabla w^{\Delta t})^T \Big\rangle_p$, where

$$D_1 = \begin{pmatrix} \frac{\Delta t}{4}(g')^2 & \frac{1}{2}(g' - f') \\ \frac{1}{2}(g' - f') & \frac{\Delta t}{4}(f')^2 \end{pmatrix}.$$

Notice the facts that $\langle \frac{1}{2}(g' - f') \rangle_p = 0$ and $\langle \nabla w^{\Delta t} \rangle_p = 0$. Therefore, we obtain

$$\begin{aligned} D^{E,\Delta t} - D^E &= D_0 (\langle \nabla w^{\Delta t} \nabla w^{\Delta t, T} - \nabla w \nabla w^T \rangle_p + O(\Delta t^2)) \\ &= D_0 \big((\nabla w^{\Delta t} - \nabla w) \nabla w^T + \nabla w (\nabla w^{\Delta t} - \nabla w)^T \\ &\quad + (\nabla w^{\Delta t} - \nabla w)(\nabla w^{\Delta t} - \nabla w)^T + O(\Delta t^2) \big). \end{aligned} \tag{65}$$

Using the results obtained in the Theorem 4.6, we can get that the order of the error in (65) is $O(\Delta t)$. ∎

THEOREM 4.8. *Let X_t denote the solution of* (15) *and X_t^{num} denote the adaptive interpolated process of* (12). *To calculate the effective diffusivity of X_t^{num}, we define $\tilde{D}^{E,num}(x,t) = E\big[\frac{(X_t^{num}-X_0)\otimes(X_t^{num}-X_0)}{2t}|X_0 = x\big]$, $0 < t \le T$. T is greater than the diffusion time, which is at most $\mathcal{O}(\sigma^{-1})$. Then, we have the estimate as follows,*

$$\sup_x |\tilde{D}^{E,num}(x,t) - D^E| \le C\Delta t + C(T)\Delta t^2. \tag{66}$$

Proof. Let $\tilde{D}^{E,\Delta t}(x,t) = E\big[\frac{(X_t^{\Delta t}-X_0^{\Delta t})\otimes(X_t^{\Delta t}-X_0^{\Delta t})}{2t}|X_0^{\Delta t} = x\big]$. If we define $\phi_0(x) = (x-X_0)^T(x-X_0)$, then Lemma 4.1 implies $|\tilde{D}^{E,num}(x,t) - \tilde{D}^{E,\Delta t}(x,t)| \le C(T)\Delta t^2$. Applying the homogenization theory (see [1, 24]), when t is large enough, $\tilde{D}^{E,\Delta t}(x,t) \to D^{E,\Delta t}$, exponetially fast. Finally, Theorem 4.7 implies $|D^{E,\Delta t} - D^E| \le C\Delta t$. Thus, the estimate (66) is obtained by using the triangle inequality. ∎

If a long-time behavior of a flow (e.g., effective diffusivity) can be approximated by a truncated flow of the numerical method, the error in quantifying such behavior may be dominated by the truncated flow that can be studied analytically. In the case of Theorem 4.8, general error analysis (see [12]) will state that $|\tilde{D}^{E,num}(x,t) - D^E| \le C(T)\Delta t$, where $C(T)$ depends on T. We obtain an improved estimate using the BEA technique. More in-depth studies on this issue will be carried out in our future work.

In our numerical experiment, we shall approximate D^E by $\tilde{D}^{E,num}$. Namely, we use the Monte Carlo method to compute the expectation in calculating the effective diffusivity. Considering that the diffusion time may depend on the molecular diffusion σ, our computational time T should depend on σ and can be bounded when calculating for a fixed σ. Thus, we can gradually decrease Δt and obtain accurate numerical results.

5. Numerical results. In this section, we shall apply our methods to investigate the behaviors of several time-dependent chaotic and stochastic flows. We are interested in understanding the mechanisms of the diffusion enhancement and the existence of residual diffusivity, highlighting the influence of Lagrangian chaos on flow transport, and comparing long-time performance of different numerical methods.

5.1. Chaotic cellular flow with oscillating vortices. We consider the passive tracer model where the velocity field is given by a chaotic cellular flow with oscillating vortices. Specifically, the flow is generated by a Hamiltonian defined as $H(t,p,q) = -\frac{1}{k}\cos(kp + B\sin(\omega t))\sin(kq)$, where k, B, and ω are parameters. The motion of a particle moving in this chaotic cellular flow is described by the SDE,

$$\begin{cases} dp = \sin(kp + B\sin(\omega t))\cos(kq)dt + \sigma dW_1, \\ dq = -\cos(kp + B\sin(\omega t))\sin(kq)dt + \sigma dW_2 \end{cases} \tag{67}$$

with initial data (p_0, q_0). When $\sigma = 0$ the behavior of (67) was intensively studied in [4], which is a two-dimensional incompressible flow representing a lattice of oscillating vortices or roll cells. Moreover, when $B = 0$ the flow in (67) turns into the Taylor–Green velocity field. In this setting real fluid elements follow trajectories that are level curves of its Hamiltonian. When $B \neq 0$, the trajectories of the passive tracers differ from the streamlines, due to the oscillating vortex in the flow. When $\sigma > 0$ the dynamics of the (67) will exhibit more structures, which is an interesting model problem to test the performance of our method.

We point out that when $B = 0$ and $\sigma > 0$, the long-time, large-scale behavior of the particle model of (67) has been studied by many researchers, for example, in

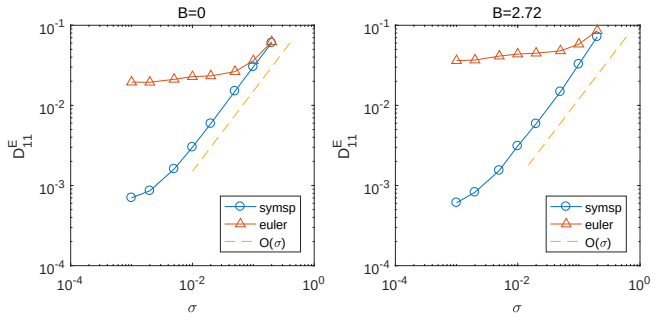

FIG. 2. *Numerical results of D_{11}^E for different σ.*

[6, 23]. It shows that the asymptotic behavior of effective diffusivity $D^E \sim \sigma I_2$ (or equivalently $D^E \sim \sqrt{2D_0} I_2$), which means that for this type of flow there does not exist residual diffusivity. We intend to study whether the residual diffusivity exists when $B \neq 0$ and $\sigma \to 0$.

In our numerical experiments, we choose $k = 2\pi$, $\omega = \pi$, $(p_0, q_0) = (0, 0)$ in the SDE (67). The time step is $\Delta t = 10^{-2}$ and the final computational time is $T = 10^4$. We consider different B to study the behaviors of effective diffusivity in vanishing viscosity (i.e., $\sigma \to 0$). We compare the numerical results obtained using the symplectic splitting scheme and Euler–Maruyama scheme. In our comparison, we use Monte Carlo samples to discretize the Brownian motions dW_1 and dW_2. The sample number is $N_{mc} = 5000$. It takes about 40 seconds to compute the effective diffusivity on a desktop with a 4-core 4.2GHz CPU (Intel Core i7-7700K). Since we only need the final state of the process to calculate D^E, memory cost only depends on the Monte Carlo sample number, which is insubstantial in our study.

In Figure 2, we show the numerical results of effective diffusivity D_{11}^E obtained using different methods and parameters. The left part of the figure shows the results for Taylor–Green velocity field ($B = 0$). One can see that the Euler–Maruyama scheme fails to achieve the theoretical analysis for D^E, i.e., $D^E \sim \sigma I_2$, while the result obtained using our symplectic splitting scheme agrees with the theory well. The right part of the figure shows the results for $B = 2.72$. One again finds that the behaviors of the Euler–Maruyama scheme and our scheme are different.

To further compare the performance of the Euler–Maruyama scheme and our method, we repeat the same experiment with $k = 2\pi$, $\omega = \pi$, $(p_0, q_0) = (0, 0)$, and $\sigma = 10^{-2}$ in (67), but try a different time step Δt with $B = 0$ and $B = 2.72$ correspondingly. In Figure 3, we find that the symplectic scheme can achieve very accurate results even using the relatively larger time step, while the Euler–Maruyama scheme cannot give the right answer even using the very smallest time step. As a result of Theorem 4.7, we can say that the numerical results for D_{11}^E have converged to the analytical result. Therefore, we conjecture that for the time-dependent cellular flow we studied in (67) with $B = 2.72$, we still have $D^E \sim \sigma I_2$. In other words, for this type of flow there does not exist residual diffusivity. More theoretical analysis of this flow will be reported in our future work.

Remark 5.1. We also test a time-dependent Taylor–Green velocity field, which is generated by the Hamiltonian defined as $H(t, p, q) = \frac{1}{k}\big(1 + B\sin(\omega t)\big)\cos(kp)\sin(kq)$, where k, B, and ω are parameters. This field can be used to model particle motion in the ocean and in the atmosphere since it contains both vortices (convection cells) and linear uprising/sinking regions [4]. Our numerical results (not shown here) indicate

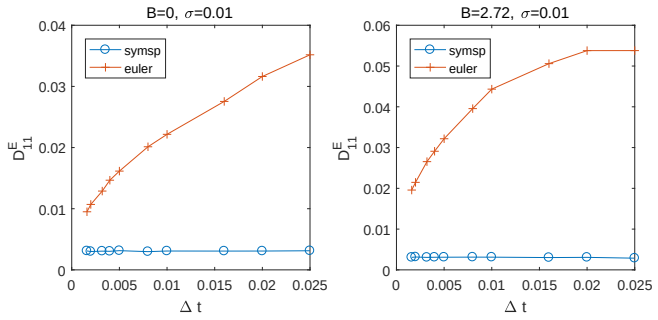

FIG. 3. *Numerical result of* D_{11}^E *for different* Δt.

that the asymptotic behaviors of effective diffusivity $D^E \sim \sigma I_2$. Namely, there does not exist residual diffusivity for this time-dependent Taylor–Green velocity field.

5.2. Investigating residual diffusivity. We now turn to another chaotic cellular flow that is generated from a Hamiltonian defined as $H(t,p,q) = \big(\sin(p) - \sin(q)\big) + \theta\cos(t)\big(\cos(q) - \cos(p)\big)$, where θ is a parameter. Then the particle path satisfies the following SDE,

$$\begin{cases} dp = \big(\cos(q) + \theta\cos(t)\sin(q)\big)dt + \sigma dW_1, \\ dq = \big(\cos(p) + \theta\cos(t)\sin(p)\big)dt + \sigma dW_2. \end{cases} \tag{68}$$

The flow in (68) is fully chaotic (well-mixed at $\theta = 1$). The first term of the velocity field $\big(\cos(q), \cos(p)\big)$ is a steady cellular flow, but the second term of the velocity field $\theta\cos(t)\big(\sin(q), \sin(p)\big)$ is a time-periodic perturbation that introduces an increasing amount of disorder in the flow trajectories as θ increases.

The flow in (68) has served as a model of chaotic advection for the Rayleigh–Bénard experiment [9]. This type of flow has been investigated numerically in [15] by solving the cell problem (48). To make the result comparable, we use D_0 as the parameter for diffusion, which is equivalent to $\frac{\sigma^2}{2}$. It was found that $D_{11}^E = O(1)$ as $D_0 \downarrow 0$, which implies the existence of the residual diffusivity. However, the solution of the advection-diffusion equation (48) develops sharp gradients as $D_0 \downarrow 0$ and demands a large amount of computational costs. We shall show that our numerical method gives comparable results that were tested in [15] with far less computational costs.

In our numerical experiments, we choose time step $\Delta t = 5 \times 10^{-2}$ and final time $T = 5 \times 10^3$ in our symplectic scheme as smaller values of Δt and larger values of T do not alter the results significantly. We use $N_{mc} = 5000$ independent Monte Carlo sample paths to discretize the Brownian motions $dW1$ and $dW2$.

In Table 1, we show the numerical results of D_{11}^E for different D_0 and θ. We also show the results in Figure 4. It takes about 20 seconds to compute one effective diffusivity for each result. We observed a *nonmonotone* dependence of D_{11}^E vs. θ in the small D_0 regime, consistent with the computation from solving cell problems in [15], though the overall trend is that D_{11}^E increases with the amount of chaos in the flows. Our numerical results again imply the existence of residual diffusivity for this type of chaotic flow. As suggested in our previous numerical investigation, the Euler–Maruyama scheme needs a much finer time step to compute the residual diffusivity and the numerical results are polluted by the diffusion of the scheme. Therefore, we do not test the Euler–Maruyama scheme in this experiment.

TABLE 1
Numerical results of D_{11}^E by the symplectic splitting scheme. The flow is defined by a chaotic cellular flow.

θ	$D_0 = 10^{-6}$	$D_0 = 10^{-5}$	$D_0 = 10^{-4}$	$D_0 = 10^{-3}$	$D_0 = 10^{-2}$	$D_0 = 10^{-1}$
0.1	0.111547	0.084047	0.068833	0.072755	0.157947	0.504085
0.2	0.176780	0.161091	0.159181	0.169005	0.213418	0.547745
0.3	1.187858	0.901204	0.521761	0.356920	0.314840	0.550539
0.4	0.457187	0.453117	0.368187	0.385328	0.422116	0.538405
0.5	0.339372	0.352455	0.326034	0.361473	0.424855	0.645214
0.6	0.268441	0.246738	0.236696	0.256992	0.394480	0.704883
0.7	0.174016	0.169134	0.176643	0.215472	0.413941	0.754199
0.8	0.677995	0.605287	0.606582	0.516210	0.533211	0.796788
0.9	1.357033	1.363832	1.373394	1.084116	0.913423	0.908773

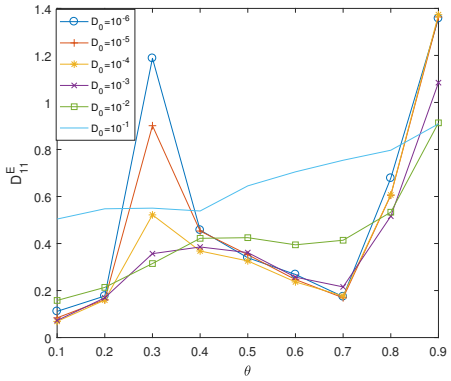

FIG. 4. *The residual diffusivity results. D_{11}^E vs. θ for the fully chaotic flow defined in* (68).

5.3. Investigating stochastic flows. We are also interested in investigating the existence of the residual diffusivity for stochastic flows. The homogenization of time-dependent stochastic flows has been studied in the literature. Under a certain integrability condition, it is proved that the effective diffusivity exists for the long-time, large-scale behavior of the solutions [7, 13]. However, there are few numerical experiments to investigate effective diffusivity quantitatively. We shall use our symplectic splitting scheme to compute the effective diffusivity for stochastic flows. More theoretical study will be reported in our subsequent paper.

The stochastic flow is constructed from the fully chaotic flow in (68), where the time-periodic function $\cos(t)$ is replaced by an Ornstein–Uhlenbeck (OU) process η_t [29]. The OU process satisfies

$$d\eta_t = \theta_{ou}(\mu_{ou} - \eta_t)dt + \sigma_{ou}dW_t^0, \tag{69}$$

where $\theta_{ou} > 0$, μ_{ou}, and $\sigma_{ou} > 0$ are parameters and dW_t^0 denotes a Brownian motion. Specifically, θ_{ou} controls the speed of reversion, μ_{ou} is the long term mean level, and σ_{ou} is the volatility or diffusion strength. In our numerical experiments, we choose $\mu_{ou} = 0$, $\theta_{ou} = 1$, and $\sigma_{ou} = 1$, so that the OU process has zero mean and the stationary variance is $\frac{\sigma_{ou}^2}{2\theta_{ou}} = \frac{1}{2}$. We choose the parameters in the OU process in such a way that its qualitative behavior is similar as $\cos(t)$. The particle path satisfies the following SDE,

$$\begin{cases} dp = (\cos(q) + \theta\ \eta_t \sin(q))dt + \sigma dW_t^1, \\ dq = (\cos(p) + \theta\ \eta_t \sin(p))dt + \sigma dW_t^2, \end{cases} \tag{70}$$

TABLE 2

Numerical results of D_{11}^E by the symplectic splitting scheme. The flow is defined by an OU process.

θ	$D_0 = 10^{-6}$	$D_0 = 10^{-5}$	$D_0 = 10^{-4}$	$D_0 = 10^{-3}$	$D_0 = 10^{-2}$	$D_0 = 10^{-1}$
0.1	0.036442	0.037821	0.042649	0.064412	0.156084	0.485647
0.2	0.070701	0.074095	0.075525	0.094416	0.172281	0.491868
0.3	0.106238	0.104986	0.112149	0.123868	0.195421	0.496326
0.4	0.137335	0.141704	0.145786	0.154876	0.221186	0.513384
0.5	0.171326	0.173708	0.176357	0.187868	0.252861	0.522133
0.6	0.197188	0.200511	0.205098	0.220810	0.272689	0.539465
0.7	0.232775	0.231468	0.240672	0.248353	0.314599	0.563992
0.8	0.259921	0.255478	0.268048	0.280238	0.332105	0.589805
0.9	0.286707	0.291560	0.290207	0.294778	0.365502	0.605338

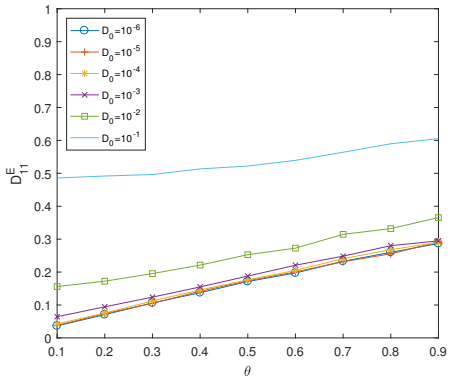

FIG. 5. *The residual diffusivity results. D_{11}^E vs. θ for the stochastic flow driven by an OU process defined in* (70).

where the Brownian motions dW_t^1 and dW_t^2 are independent from the one used in the definition of the OU process (69).

Since the OU process has an ergodic property, we choose a small amount of sample paths, say, $n_{ou} = 100$, and final computational time $T = 5 \times 10^3$ to compute the effective diffusivity. In Table 2, we show the numerical results of D_{11}^E for different D_0 and θ, where each D_{11}^E is the average values obtained from the n_{ou} paths. In Figure 5, we show the results corresponding to Table 2. It takes about 20 seconds to compute one effective diffusivity result for each OU path. The total computational time can be estimated accordingly. We observed a *monotone* dependence of D_{11}^E vs. θ in this example. Our numerical results again imply the existence of residual diffusivity for this type of stochastic flow. We observe however that the nonmonotonic dependence in θ disappears. Namely, the residual diffusivity is an increasing function of θ. Such a phenomenon a is due to the absence of resonance in stochastic flows.

Furthermore, we show the ergodicity results of the effective diffusivity in Figure 6. In this test, we choose the parameters $\theta = 0.1$, $D_0 = 10^{-2}$ and compute the effective diffusivity along 100 OU paths. We show the histogram of $D^E(\omega_{OU})$ at $T = 100$, $T = 200$, $T = 500$, $T = 5000$, and $T = 20000$, respectively. Notice that for each OU path (i.e., one realization of η_t defined in (69)), we use $N_{mc} = 1000$ independent Monte Carlo sample paths to discretize the Brownian motions dW_t^1 and dW_t^2 defined in (70). The Figure 6 shows two facts: first, as the computational

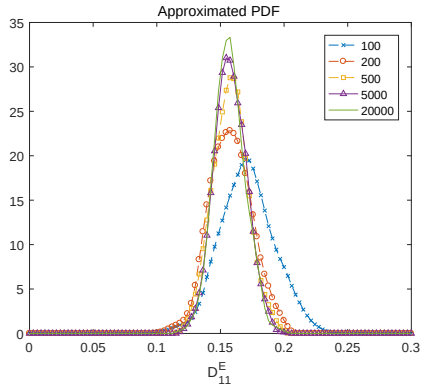

FIG. 6. *Histogram of the residual diffusivity results.* D_{11}^E *for the stochastic flow driven by an OU process defined in* (70) *that are computed at different final times.*

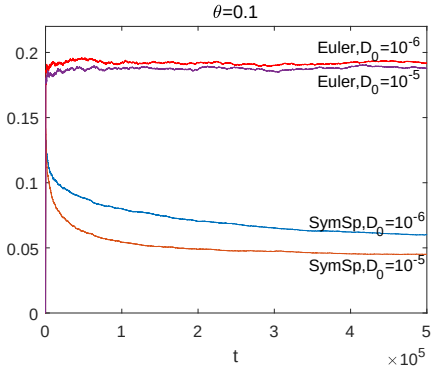

FIG. 7. *Behavior of* $\frac{\langle (x_1(t)-x_1(0))^2\rangle}{2t}$ *as a function of time for two different methods.*

time becomes long enough the histogram appears to converge to a limit distribution. The limit distribution has much smaller variance and is centered closer to 0.156084. Second, in Table 1 we show the residual diffusivity obtained from the fully chaotic (well-mixed) flow. When the parameters $\theta = 0.1$, $D_0 = 10^{-2}$, the corresponding residual diffusivity is $D_{11}^E = 0.157947$. Thus, the chaotic and stochastic flows may share some similar mechanism in their long-time behaviors. More theoretical and numerical investigations will be studied in our future work.

5.4. Behaviors of the long-time integration. Theorem 4.2 proves that the symplectic splitting scheme preserves the asymptotic Hamiltonian structure that enables us to compute the stable long-time behavior of the effective diffusivity of chaotic and stochastic flows. We now keep using the flow (68) and compute a much longer time solution with final time $T = 5 \times 10^5$.

In Figure 7, we plot the calculated effective diffusivity D_{11}^E as a function of time obtained using different methods and parameters. The two lines on the top are corresponding to the Euler–Maruyama method for $D_0 = 10^{-5}$ and $D_0 = 10^{-6}$, while the two lines on the bottom are corresponding to the symplectic splitting method. It is clear that results obtained from the symplectic splitting method converge to a more stable value. A probable explanation is that the solution obtained using the symplec-

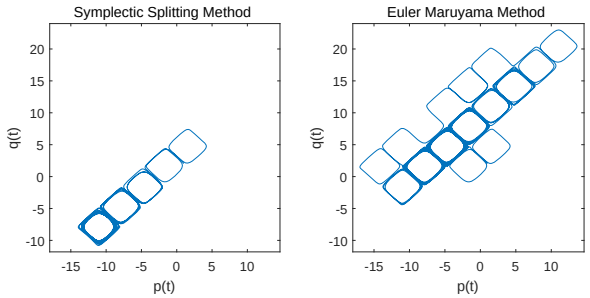

FIG. 8. *Phase plane for the two different methods.*

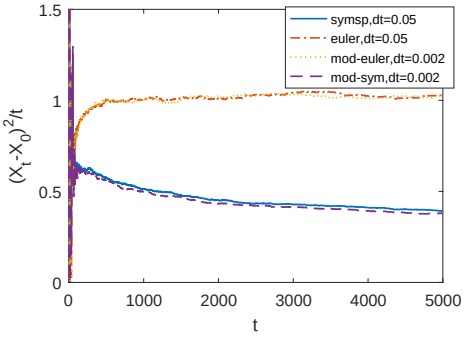

FIG. 9. *Behavior of* $\frac{\langle (x_1(t)-x_1(0))^2\rangle + \langle (x_2(t)-x_2(0))^2\rangle}{t}$ *for two different methods with* $\theta = 0.3$ *and* $D_0 = 10^{-5}$.

tic splitting scheme follows an asymptotic Hamiltonian, while the solution obtained using Euler method does not, which has been proved in the Theorem 4.2.

Additional evidence comes from Figure 8, where we plot the phase plane for two different numerical methods. The realization of the noise is the same and we integrated up to time $T = 10^3$ with time step $\Delta t = 0.05$. We choose the parameters $\theta = 0.1$ and $D_0 = 10^{-5}$. From these results, we find that the paths oscillate near a line with slope 1. It is clear that the behaviors of two methods are different. In the case of the Euler–Maruyama method, the particle appears to be more diffusive than that in the symplectic splitting scheme.

In Figure 9, we show how the modified equation approximates the original problem, where we consider the chaotic cellular flow (68). More specifically, we plot the effective diffusivity $2(D_{11}^E + D_{22}^E)$ as a function of time obtained using different methods and we choose the parameter $\theta = 0.3$ and $D_0 = 10^{-5}$. From our numerical results, we find that the effective diffusivity obtained using our method with time step $\Delta t = 0.05$ agrees very well with the one obtained by solving the modified equation using the Euler–Maruyama method with time step $\Delta t = 0.002$. Namely, we approximately achieve a $25X$ speedup over the Euler–Maruyama method. The Euler–Maruyama method with $\Delta t = 0.05$ also generates results that agrees with its corresponding modified equation with a finer time step. But the effective diffusivity converges to a wrong result.

6. Conclusions. Quantifying diffusion enhancement in fluid advection is a fundamental problem that has many applications in physical and engineering sciences.

We proposed an effective structure-preserving scheme that can efficiently compute the effective diffusivity of chaotic and stochastic flows containing complex streamlines. In addition, we investigate the existence of the residual diffusion phenomenon in chaotic and stochastic advection, which is an interesting problem by itself. The effective diffusivity as well as the residual diffusivity can be computed by solving the Fokker–Planck equation in the Eulerian formulation. However, when the molecular diffusion parameter becomes small, the solutions of the advection-diffusion equation develop sharp gradients and thus demand a large amount of computational costs.

We compute the effective diffusivity in the Lagrangian formulation, i.e., solving SDEs. We split the original problem into a deterministic subproblem and a random perturbation, where the former is discretized using a symplectic preserving scheme while the later is solved using the Euler–Maruyama scheme. We provide rigorous error analysis for our new numerical integrator using the BEA technique and show that our method outperformed standard Euler-based integrators. Numerical results are presented to demonstrate the accuracy and efficiency of the proposed method for several typical chaotic and stochastic flows problem of physical interest. We find that the residual diffusivity exists in some time periodic and stochastic cellular flows.

There are two directions we want to explore in our future work. First, we shall investigate the existence of the residual diffusivity for other stochastic flows and develop convergence analysis for the corresponding numerical methods. In addition, we shall study other issues to improve the efficiency of our methods, such as developing an adaptive time-stepping method and using the multilevel Monte Carlo method to reduce the sample number in our method.

REFERENCES

[1] A. Bensoussan, J.-L. Lions, and G. Papanicolaou, *Asymptotic Analysis for Periodic Structures*, AMS, Providence, RI, 2011.

[2] L. Biferale, A. Crisanti, M. Vergassola, and A. Vulpiani, *Eddy diffusivities in scalar transport*, Phys. Fluids, 7 (1995), pp. 2725–2734.

[3] N. Bou-Rabee and H. Owhadi, *Long-run accuracy of variational integrators in the stochastic context*, SIAM J. Numer. Anal., 48 (2010), pp. 278–297.

[4] J. Cartwright, U. Feudel, G. Karolyi, A. Moura, and O. Tamas Tel, *Dynamics of finite-size particles in chaotic fluid flows*, in Nonlinear Dynamics and Chaos: Advances and Perspectives, Springer, Berlin, 2010, pp. 51–87.

[5] L. C. Evans, *Partial Differential Equations*, AMS, Providence, RI, 2010.

[6] A. Fannjiang and G. Papanicolaou, *Convection-enhanced diffusion for periodic flows*, SIAM J. Appl. Math., 54 (1994), pp. 333–408.

[7] A. Fannjiang and G. Papanicolaou, *Convection-enhanced diffusion for random flows*, J. Stat. Phys., 88 (1997), pp. 1033–1076.

[8] J. Garnier, *Homogenization in a periodic and time-dependent potential*, SIAM J. Appl. Math., 57 (1997), pp. 95–111.

[9] A. V. Getling, *Rayleigh–Bénard Convection: Structures and Dynamics*, Adv. Ser. Nonlinear Dynam. 11, World Scientific, River Edge, NJ, 1998.

[10] E. Hairer, C. Lubich, and G. Wanner, *Geometric Numerical Integration: Structure-Preserving Algorithms for Ordinary Differential Equations*, Springer, Berlin, 2006.

[11] V. V. Jikov, S. Kozlov, and O. A. Oleinik, *Homogenization of Differential Operators and Integral Functionals*, Springer, Berlin, 1994.

[12] P. E. Kloeden and E. Platen, *Numerical Solution of Stochastic Differential Equations*, Springer, Berlin, 1992.

[13] C. Landim, S. Olla, and H. Yau, *Convection–diffusion equation with space–time ergodic random flow*, Probab. Theory Related Fields, 112 (1998), pp. 203–220.

[14] Y. Liu, J. Xin, and Y. Yu, *Asymptotics for turbulent flame speeds of the viscous G-equation enhanced by cellular and shear flows*, Arch. Ration. Mech. Anal., 202 (2011), pp. 461–492.

[15] J. Lyu, J. Xin, and Y. Yu, *Computing residual diffusivity by adaptive basis learning via spectral method*, Numer. Math. Theory Methods Appl., 10 (2017), pp. 351–372.

[16] A. Majda and K. Peter, *Simplified models for turbulent diffusion: Theory, numerical modelling, and physical phenomena*, Phys. Rep., 314 (1999), pp. 237–574.
[17] R. I. McLachlan and G. R. Quispel, *Splitting methods*, Acta Numer., 11 (2001), pp. 341–434.
[18] G. Milstein, Y. Repin, and M. Tretyakov, *Symplectic integration of Hamiltonian systems with additive noise*, SIAM J. Numer. Anal., 39 (2002), pp. 2066–2088.
[19] B. Oksendal, *Stochastic Differential Equations: An Introduction with Applications*, Springer, Berlin, 2013.
[20] G. Pavliotis and A. Stuart, *White noise limits for inertial particles in a random field*, Multiscale Model Simul., 1 (2003), pp. 527–553.
[21] G. Pavliotis and A. Stuart, *Periodic homogenization for inertial particles*, Phys. D, 204 (2005), pp. 161–187.
[22] G. Pavliotis and A. Stuart, *Homogenization for inertial particles in a random flow*, Commun Math Sci., 5 (2007), pp. 507–531.
[23] G. Pavliotis, A. Stuart, and K. Zygalakis, *Calculating effective diffusivities in the limit of vanishing molecular diffusion*, J. Comput. Phys., 228 (2009), pp. 1030–1055.
[24] G. A. Pavliotis and A. Stuart, *Multiscale Methods: Averaging and Homogenization*, Springer, Berlin, 2008.
[25] S. Reich, *Backward error analysis for l integrators*, SIAM J. Numer. Anal., 36 (1999), pp. 1549–1570.
[26] H. Risken, *The Fokker-Planck Equation*, Springer Ser. Synergetics, Springer, Berlin, 18, 1989.
[27] G. Strang, *On the construction and comparison of difference schemes*, SIAM J. Numer. Anal., 5 (1968), pp. 506–517.
[28] M. Tao, *Explicit symplectic approximation of nonseparable Hamiltonians: Algorithm and long time performance*, Phys. Rev. E, 94 (2016), 043303.
[29] G. E. Uhlenbeck and L. S. Ornstein, *On the theory of the Brownian motion*, Phys. Rev., 36 (1930), 823.
[30] L. Wang, J. Hong, and L. Sun, *Modified equations for weakly convergent stochastic symplectic schemes via their generating functions*, BIT, 56 (2016), pp. 1131–1162.
[31] P. Zu, L. Chen, and J. Xin, *A computational study of residual KPP front speeds in time-periodic cellular flows in the small diffusion limit*, Phys. D, 311 (2015), pp. 37–44.
[32] K. Zygalakis, *On the existence and the applications of modified equations for stochastic differential equations*, SIAM J. Sci. Comput., 33 (2011), pp. 102–130.